RESEARCH INTO DRIVE SYSTEM OF EOD/IED ROBOT

Tomasz Muszyński

Military University of Technology, Faculty of Mechanical Engineering
Department of Construction Machinery
Gen. S. Kaliskiego Street 2, 00-908 Warsaw, Poland
tel.+48 22 6837107, fax: +48 22 6837211
e-mail: tmuszynski@wat.edu.pl

Abstract

Navigating vehicles over difficult terrain requires a drive system ensuring high mobility. It is particularly important in the case of unmanned ground vehicles. It is often not realized that a vehicle occupant frequently plays the role of a multi sensor, highly effective data processor and a control system at the same time. Due to this, the abilities of an unmanned vehicle's drive system should, to the greatest possible extent, compensate for the lack of an inside operator. To achieve this, it has to ensure high precision and ease of controlling. Such possibilities are provided by electric and hydrostatic systems.

At the Military University of Technology, Chair of Engineering Equipment, a test platform for an EOD/IED robot was developed. Due to its considerable weight, it was equipped with a hydrostatic drive system. The vehicle has a six-wheeled chassis and a skid steering system. The paper presents initial findings of the research aimed at determining the influence of the applied hydraulic system solution on the appearance of kinematic incompatibilities.

The presented experimental research included the identification of internal resistance as well as tests on three types of surfaces.

Keywords: unmanned ground vehicles, hydrostatic drive, high mobility

1. Introduction

The effectiveness of tasks conducted by unmanned ground vehicles depends largely on the features of their drive systems. It particularly concerns constructions intended for work in difficult terrain conditions, i.e. low-bearing capacity surfaces, terrain with low adhesion coefficient and with high driving resistance. In the case of a wheel traction system, it can be ensured only by independent all-axle drive. However, the latter results in the appearance of kinematic incompatibilities and in a circulating power effect. In order to prevent it, various solutions are applied which enable controlled speed differentiation of particular wheels. In mechanical drive systems it is ensured by limited slip differentials or locking differentials as well as by viscous couplings. Such solutions are applied in most off-road vehicles.

However, unmanned ground vehicles are dominated by electric and hydrostatic drive systems, with motors mounted directly in wheels. It is due to the greater ease of controlling and to the simpler and more flexible structure.

Work is underway at the Chair of Engineering Equipment of the Military University of Technology on various types of robots and one of the outcomes is a test platform for an EOD/IED robot (Fig. 1). The high requirements as regards the ability to move in off-road conditions resulted in the application of a six-wheel running gear. Due to the vehicle's gross weight of 3 500 kg, a hydrostatic drive system was selected. It has two running modes:

I - road (Fig. 2a),
II – off-road (Fig. 2b).

Fig. 1. EOD/IED robot developed at Chair of Engineering Equipment of Military University of Technology [1]
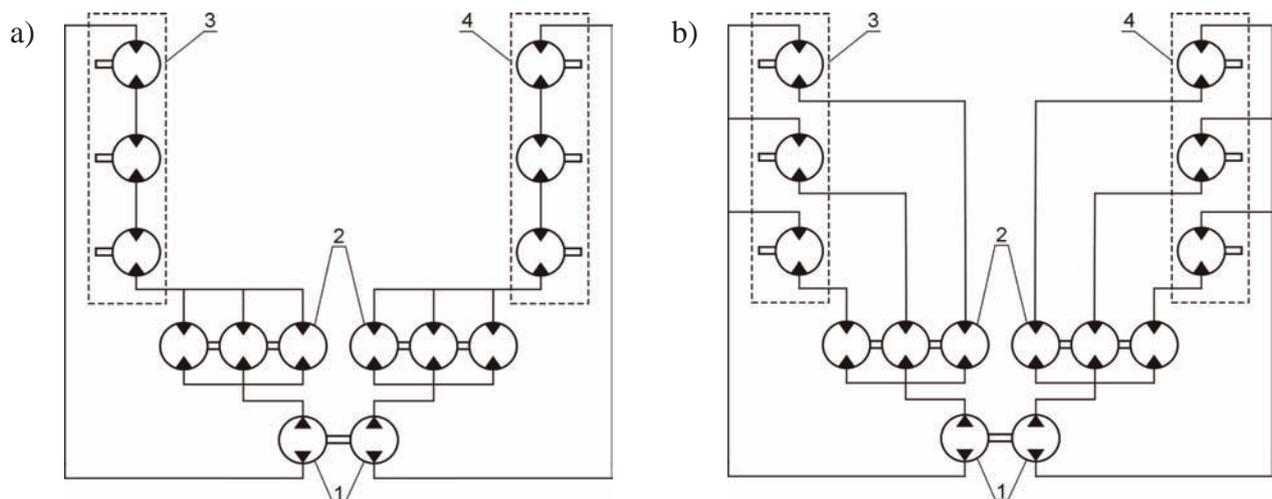
Fig. 2. Schematic diagram of hydrostatic drive system of EOD/IED robot: a) road running mode, b) off-road running mode, where: 1 – drive motors of left side wheels, 2 – drive motors of right side wheels, 3 – drive system feed pump, 4 – flow switches

In each mode, the drive is constantly transferred to all wheels, irrespective of the differences in the driving and adhesion resistance. The road mode ensures capability of high driving force. In this mode the hydraulic motors are powered independently by respective switch sections, which can be accompanied by pressure drops across the motors, equivalent to the difference between the maximum working pressure and the pressures of the installation internal resistance forces (Fig.3a). By contrast, in the road-running mode it is possible for the robot to reach its maximum speed ($v_{II\,max} \approx 30$ km/h) at the expense of decreasing the drive force. In such a case the motors are connected in series and across each one of them there is a pressure drop equivalent to approximately ⅓ of the total pressure value (Fig. 3b).

The robot is manoeuvred by means of skid steering. The use of a bidirectional pump of variable efficiency resulted in the achievement of an infinitely variable turning radius. Because of the "push-pull" feeding mechanism of its left and right sides, the vehicle is capable of a counter rotational turn. This feature is very important since it facilitates the control of the vehicle in the system of teleoperation.
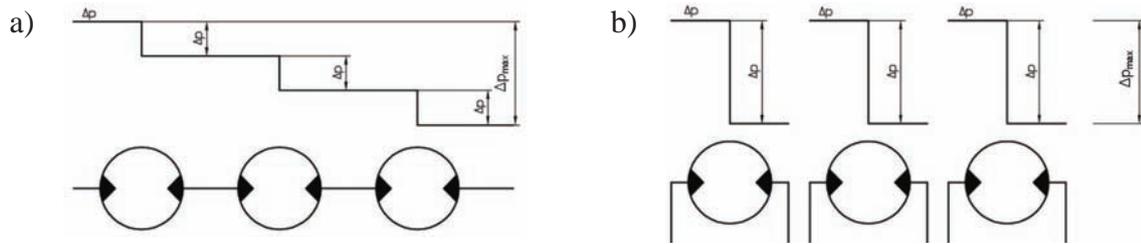
Fig. 3. Graphical interpretation of pressure drop in hydraulic motors, which drive wheels on one side of the vehicle : a) series connection, b) parallel connection [2]

In order to evaluate processes occurring in the hydraulic installation in the presence of a permanent all-wheel drive transmission, experimental tests were conducted. Their main aim was to determine the effects of the appearance of kinematic incompatibilities. The paper presents findings of the research connected to the identification of hydraulic system internal resistance forces and to moving on surfaces of various bearing capacity in the off-road running mode.

2. Measurement system

In the course of the measurement pressure variations in the feed and return lines as well as rotational speeds in the hydraulic motors of the right-side wheels were recorded. The measurement system consisted of the following elements (Fig. 4):

a) KOBOLD SEN-8700 pressure sensors:
   - front wheel: feed line – measurement range 0—600 bars,
       measurement class 0.5;
       return line – measurement range 0 – 400 bars,
       measurement class 0.5;
   - middle wheel: feed line – measurement range 0—400 bars,
       measurement class 0.5;
       return line – measurement range 0 – 600 bars,
       measurement class 0.5;
   - rear wheel: feed line – measurement range 0—400 bars,
       measurement class 0.5;
       return line – measurement range 0 – 600 bars,
       measurement class 0.5;
b) RHEINTACHO Messtechnik sensors of wheel rotational speed, mounted directly in hydraulic motors, with a frequency output of 0,1Hz – 20 kHz, 80Hz – 1 rotation/1s,
c) IO Tech Personal DAQ 3005 data acquisition board,
d) data recording computer.

The adapted notation of measured signals, which is used hereinafter, is shown in Table 1.

Tab. 1. Adapted notation system of measured parameters

	SENSOR LOCATION		ADAPTED NOTATION
PRESSURE SENSORS	rear wheel	feed line	S1
		return line	S2
	middle wheel	feed line	S3
		return line	S4
	front wheel	feed line	S5
		return line	S6
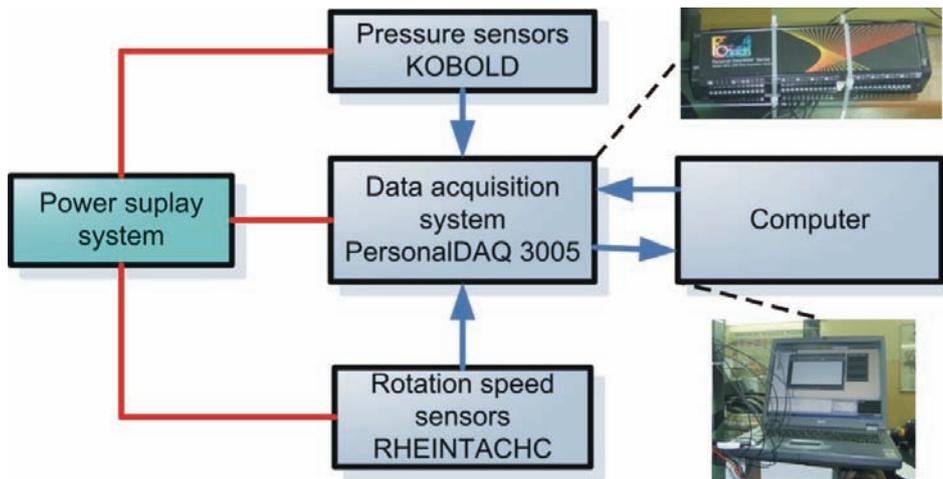
Fig. 4. Flowchart of measurement system arrangement

3. Internal resistance of hydraulic drive system

The determination of hydraulic installation internal resistance served as the basis for determining actual motion resistance forces and enabled the verification of the analytical calculations. The measurement consisted in recording the feed line (S1, S3, S5) and return line (S2, S4, S6) pressures, with an "unloaded" drive system. The latter was achieved by lifting all of the robot's wheels off the surface (Fig. 5).
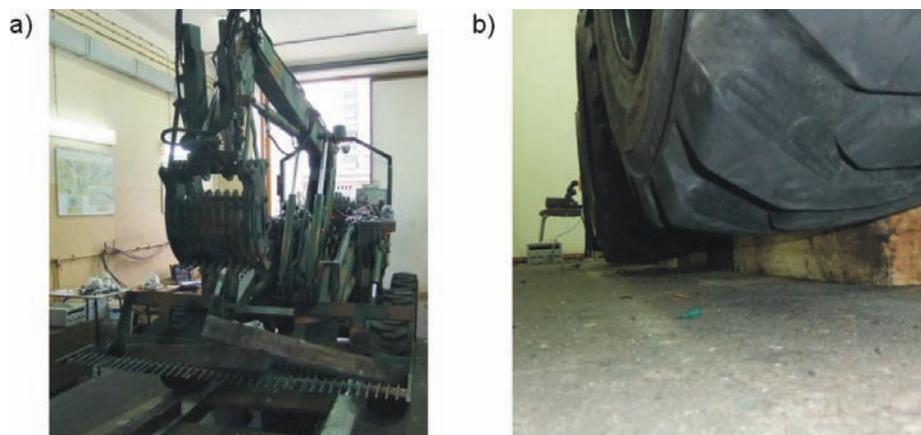
Fig. 5. EOD/IED robot during tests on drive system internal resistance: a) general view during the test, b) view illustrating lack of contact between the wheels and the surface

The test consisted in increasing, gradually, the rotational velocity of the wheels, from 0 to its maximum value. The time graphs of pressure variations across particular lines are shown in Fig. 6 and Fig. 7.

The analysis of the time graphs shown in Fig. 6 makes it possible to conclude that, in the case of idle running, the pressure across the S1 line is at its lowest and equals $\Delta p_{S1} \approx 25$ bars. Across the S3 line it is slightly higher and reaches approximately $\Delta p_{S3} \approx 27$ bars. However, the value of $\Delta p_{S5} \approx 35$ bars, obtained for the S5 line, is significantly different from the both. These differences disappear once the driving wheels are set in motion. Such an effect results from the use of the S5 line as a control signal source for other elements of the hydraulic system. Since the signal is transmitted hydraulically, there appear leaks when the pressure is low.

The increase in the velocity of the wheels is accompanied by a pressure increase in all the lines, from $\Delta p \approx 35$ bars to $\Delta p \approx 46$ bars and, in impulses, even up to $\Delta p \approx 56$ bars. Thus, it is an increase of approximately 30-60%.
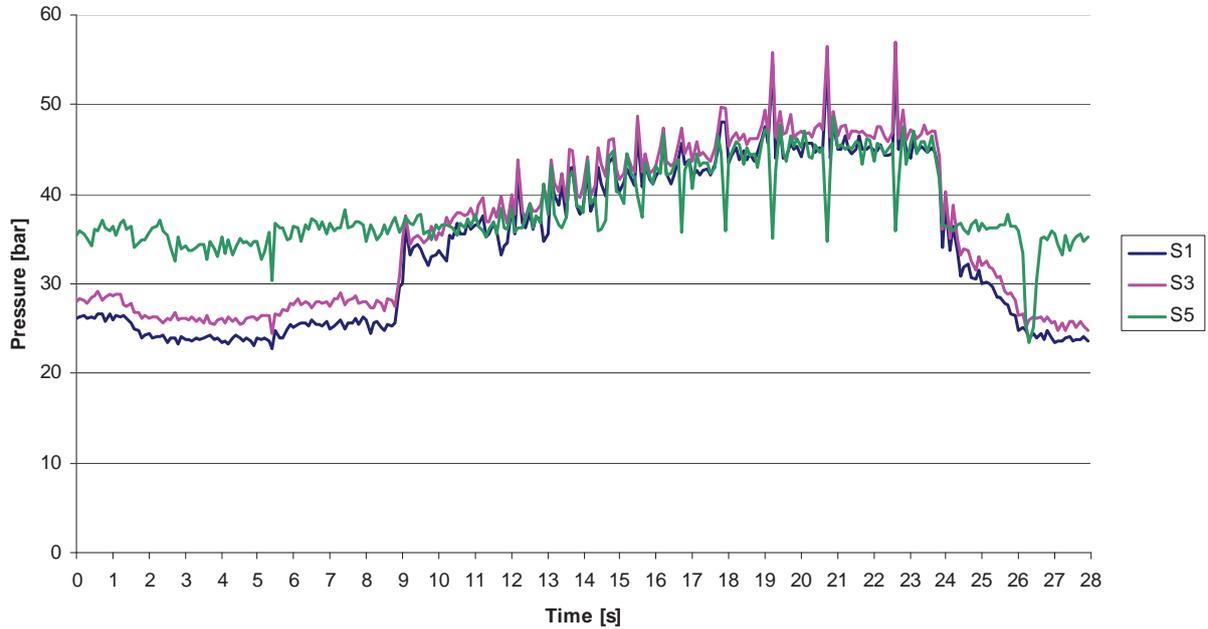
Fig. 6. Time graphs of pressure variations across feed lines of wheel drive motors in the course of tests on drive system internal resistance
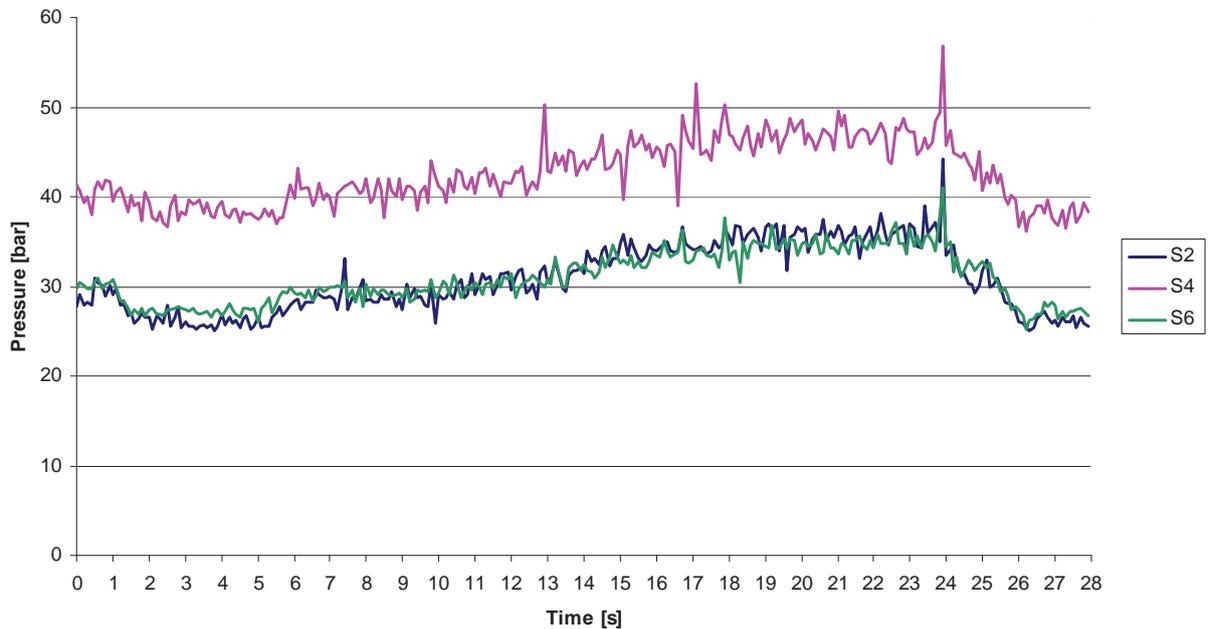
Fig. 7. Time graphs of pressure variations across return lines of wheel drive motors in the course of tests on drive system internal resistance

In the return lines (Fig. 7) the pressure variations are identical for both the front and rear wheels. In the case of idle running they are $\Delta p_{S2} \approx \Delta p_{S6} \approx 27$ bars, whereas in the case of the maximum rotational velocity of the wheels, they increase to $\Delta p_{S2} \approx \Delta p_{S6} \approx 35$ bars. Although in the S4 line the character of pressure variations is the same as in the two other lines, its pressure values are approximately 10 bars higher. This difference results from the use of a hydraulic cable of different diameter, which was dictated by constructional reasons.

4. Drive system loads

The findings presented in this part of the paper were recorded during straight-line drive tests at idle running. The tests were run on three types of surfaces:
a) asphalt surface (Fig. 8);
b) natural ground with bearing capacity of CI = 280 kPa (Fig. 9);
c) natural ground with bearing capacity of CI = 150 kPa (Fig. 10).

The timings recorded during running on the asphalt surface (Fig. 8) are almost identical across all the lines. In the course of a constant velocity drive ($v \approx 5$km/h), the pressure value remains within the range of $\Delta p \approx 100\text{-}120$ bars. At the extreme, they reached $\Delta p \approx 150$ bars and it was in the course of starting to move. Across the return lines, the pressures reached values similar to the ones recorded during the internal resistance tests although they display momentary increases of up to $\Delta p \approx 50$ bars. Such an effect was observed when the operator sharply decreased the pump efficiency to the level below hydraulic motors' demand. It was then that the motors switched to the braking mode, which was indicated by pressure increase across the return lines. In particular, it can be seen in the final part of the time graph, where the pressures reached values exceeding those across the feed lines.
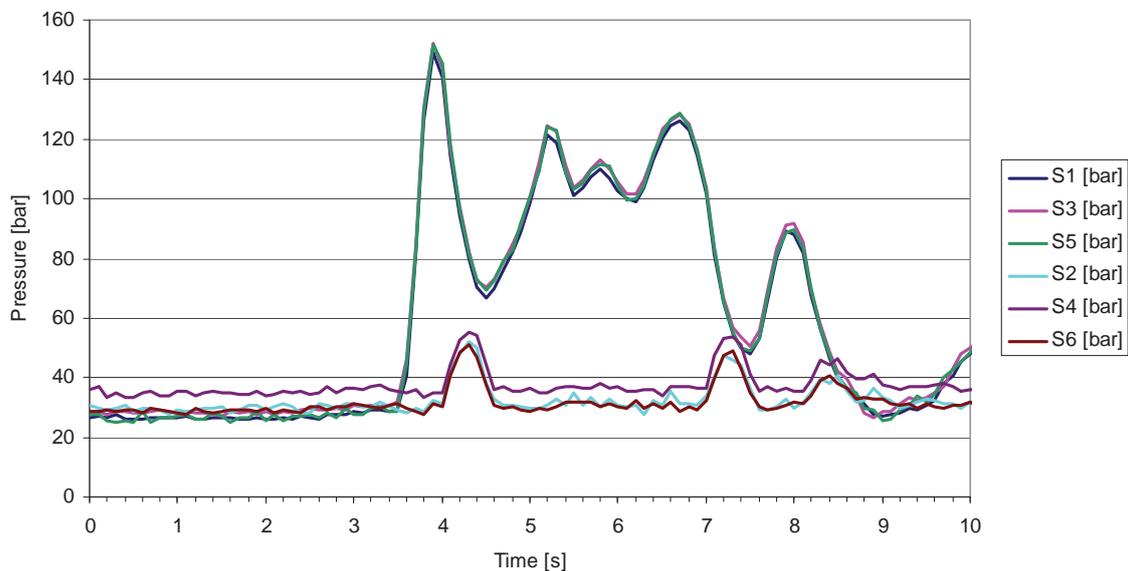
Fig. 8. Time graphs of pressure variations across feed and return lines of hydraulic motors during robot's drive on asphalt surface

In the course of running on natural ground with the bearing capacity of CI = 280 kPa (Fig. 9) at a constant velocity, the pressure across the feed lines remains within the range of $\Delta p \approx 60\text{-}80$ bars. In the course of starting to move, it rose up to $\Delta p \approx 120$ bars. Therefore, generally the values are approximately 30% lower than in the case of running on the asphalt surface. It is related to the lower soil cohesion and, thus, to the increased skids of the wheels. The time graphs for all three wheels are identical, which confirms regularity of the drive forces that they generate.

The picture of pressure variations across the return lines is also analogous to what was observed during running on the asphalt surface. The effect of braking, by means of the hydraulic motors, is clearly seen in the final part of the time graph. It was then that the pressure increased to approximately $\Delta p \approx 90$ bars and it was definitely higher than across the feed lines ($\Delta p \approx 22$ bars).

The time graph shown in Fig.10, obtained during tests on the surface with the lowest bearing capacity (CI=150 kPa), can be divided into two parts. The first one, lasting approximately 9 seconds, reflects driving with visible kinematic differences. Such a case can be seen between 1,4 and 2,8 seconds in the case of the S5 line. It is there that the pressure drops below the values observed across the S1 and S3 lines, which attests the skidding of the wheel. It results from high

motion resistance ($\Delta p \approx 150\text{-}210$ bars) accompanied by low surface cohesion. At the same time, there is no indication that it translates into different pressure timing values. It may result from the efficiency of the applied switches. A similar effect can be seen in 7,6 second in the case of the S1 line.

In the second part of the time graph (after 9 second) all the motors were evenly loaded. The pressure ranged between $\Delta p \approx 100\text{-}150$ bars. Thus, it was slightly higher than in the case of running on the asphalt surface.
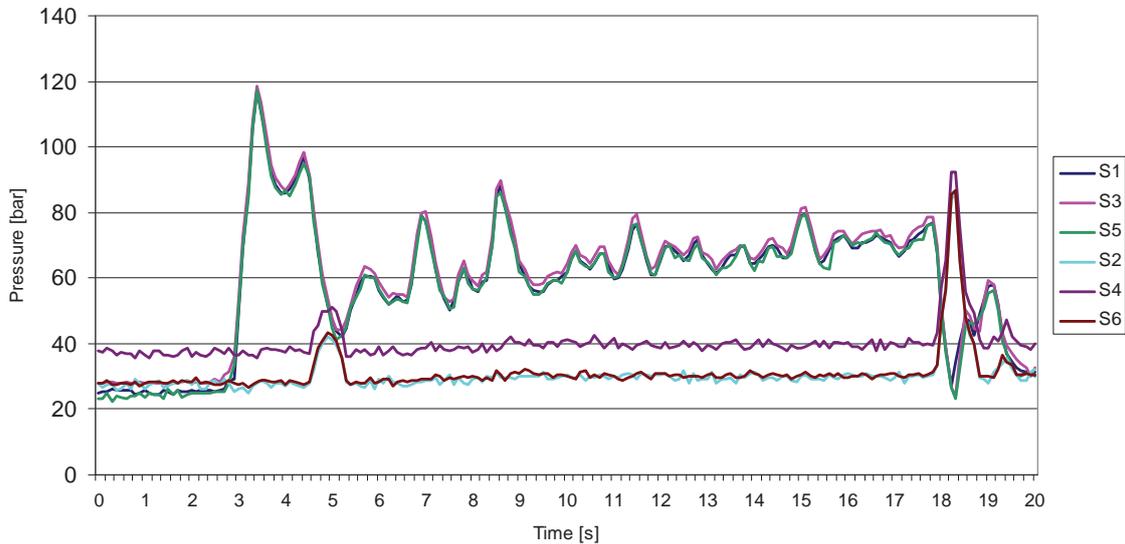
Fig. 9. Time graphs of pressure variations across feed and return lines of hydraulic motors in the course of running on natural ground with bearing capacity of CI = 280 kPa
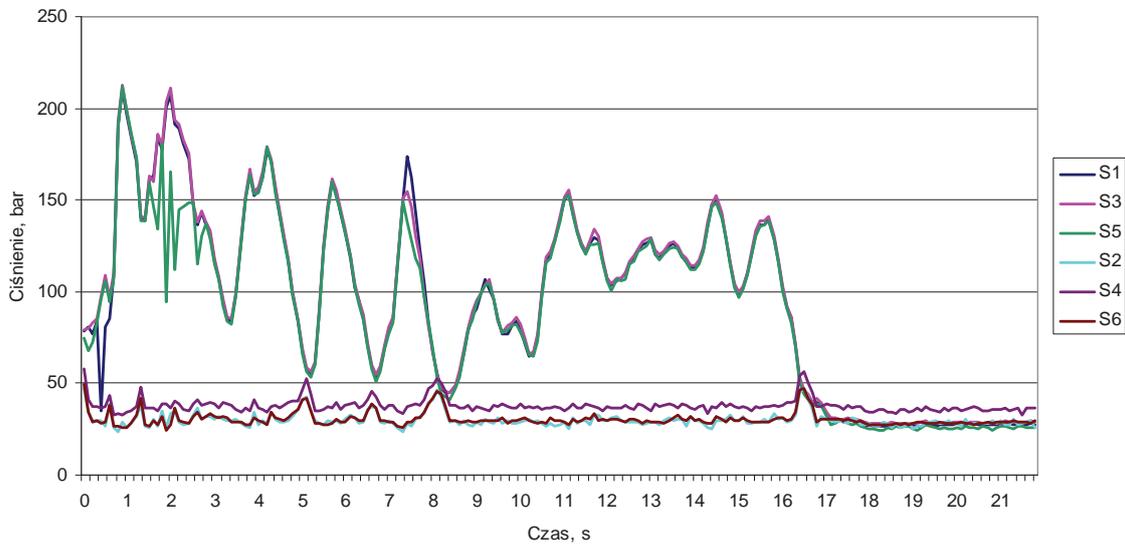
Fig. 10. Time graphs of pressure variations across feed and return lines of hydraulic motors in the course of running on natural ground with bearing capacity of CI = 150 kPa

5. Summary

During the performed tests on driving in a straight line it was concluded that the hydrostatic drive system of the EOD/IED robot, developed at the MUT Chair of Engineering Equipment, did not generate significant kinematic variations. The loading forces of the hydraulic motors, in the case of driving at a constant velocity, were within the range of $\Delta p \approx 60\text{-}150$ bars. Extreme values of the recorded pressure appeared in the course of starting to move and they reached approximately $\Delta p \approx 210$ bars.

In the case of high bearing capacity surfaces, no difference was observed as regards drive forces across particular wheels. This indicates the lack of kinematic differences. Even though such an effect was observed in the case of the low bearing capacity surface, it did not cause significant pressure variations in the system.

Across the return lines the pressures did not exceed $\Delta p \approx 30\text{-}40$ bars and they increased only during braking by means of the hydraulic motors. It was then that they raised maximally to approximately $\Delta p \approx 90$ bars.

In the course of the research tests it was determined that the drive system nominal pressure value of 320 bars was not exceeded.

References

[1] Łopatka, M. J., Praca zbiorowa, *Inżynieryjny Robot Wsparcia IOD/EOD - usuwania ładunków i ładunków niebezpiecznych,* Sprawozdanie z projektu rozwojowego Nr OR00001205/PBR, Warszawa 2011.

[2] Bartnicki. A., Muszyński. T., *Koncepcja układu napędowego dla bezzałogowej platformy lądowej o skręcie burtowym*, Międzynarodowa Konferencja Naukowo-Techniczna Napędy i Sterowania Hydrauliczne i Pneumatyczne, Wrocław 2010.